CHAPTER 4

OPTIMUM MAGNETIC FIELD PROFILE FOR THE PARALLEL PLATE POROUS SLIDER

In the last chapter we saw the use of magnetohydrodynamic effects to increase the load capacity of bearings with liquid metal lubricants. In many cases the increase in load capacity is achieved at the expense of increased frictional force, because any decrease in frictional force usually requires an expenditure of electrical energy.

An interesting problem in hydromagnetic lubrication is to determine the optimum geometric shape of the film or the optimum magnetic field profile. Osterle and Young [50] showed that the optimum geometric shape for the magnetohydrodynamic slider bearing with a uniform transverse magnetic field was a step function with riser location and step height ratio depending on the strength of magnetic field. Agrawal [51] considered the optimum geometric shape for the hydromagnetic slider bearing with a tangential magnetic field and found that it was also a step function with riser location and step height ratio depending on the magnetic field. In the above investigations the magnetic field was assumed to be uniform.

Kuzma [52] and Ramanaiah [53] considered the magnetohydrodynamic parallel plate slider bearings with non-uniformly applied transverse and tangential magnetic fields respectively. They showed that the optimum magnetic field profile was a step function with the step location and step height ratio depending on the maximum field strength. It was found that this profile increased the load capacity and decreased the friction factor and further that the parallel plate slider bearing with a non-uniform magnetic field was superior to that with a uniform magnetic field [52].

All the above investigators assumed that the slider and the bearing were impermeable. In this chapter we determine the optimum transversely applied magnetic field profile for the parallel plate slider bearing where the bearing has a porous facing backed by a solid wall.

4.1 Mathematical formulation

Consider an infinitely long slider bearing having length A along the x-axis, constant film thickness $h = h_1$ along the y-direction and a transverse applied magnetic field $B_0(x)$. The non-conducting slider moves with a uniform velocity U in the x-direction (Fig. 11). The stator is made of a material with high electrical conductivity so that short circuit conditions may be assumed. It has a porous facing of thickness H which is backed by a solid wall. Following the assumptions of porous metal hydromagnetic lubrication, the basic equations governing the flow of the lubricant in different regions are as follows :

Film region :

$$\frac{\partial^2 u}{\partial y^2} - \frac{M^2}{h^2} u = \frac{1}{\mu} \frac{dp}{dx} \tag{1}$$

$$\frac{\partial u}{\partial x} + \frac{\partial v}{\partial y} = 0 \tag{2}$$

Porous region :

$$V_x = -\frac{k}{\mu} \frac{\partial P}{\partial x} \frac{1}{c^2} \tag{3}$$

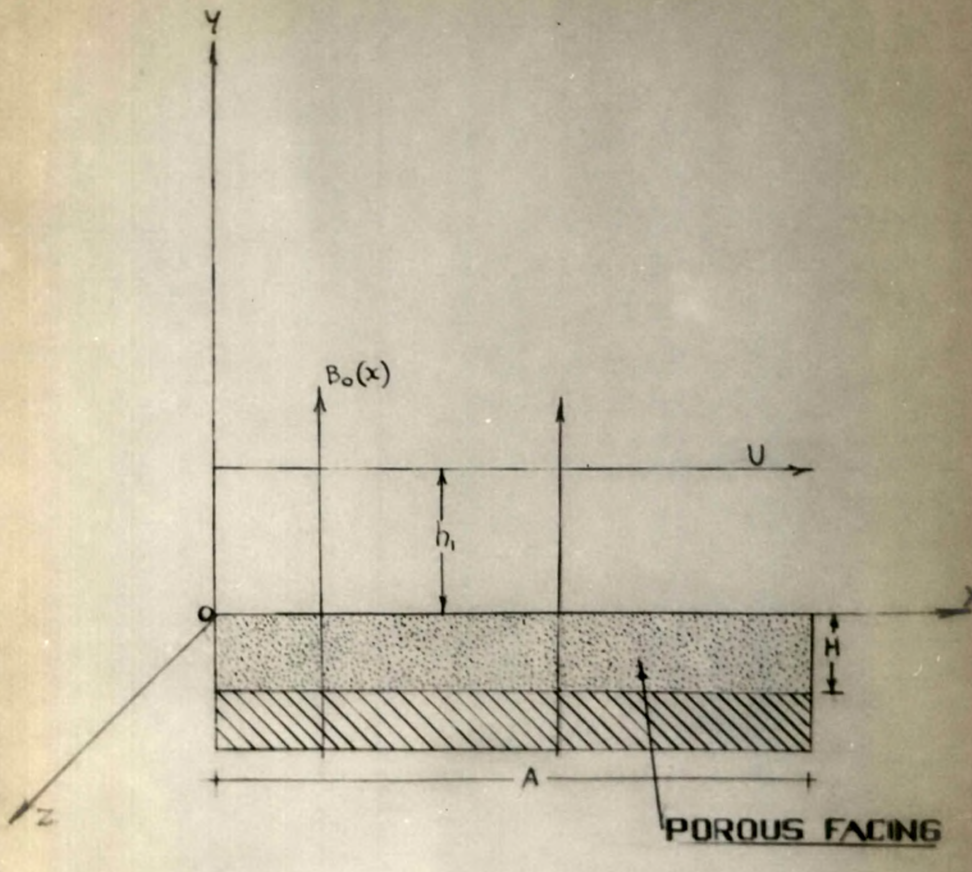

FIG. 11. PARALLEL PLATE POROUS SLIDER WITH A VARIABLE MAGNETIC FIELD.

$$V_y = - \frac{k}{\mu} \frac{\partial P}{\partial y} \qquad (4)$$

$$\frac{\partial V_x}{\partial x} + \frac{\partial V_y}{\partial y} = 0 \qquad (5)$$

where

$$c = \left(1 + \frac{k}{m^*} \frac{M^2}{h_1^2}\right)^{1/2} \text{ and } M = B_0 h_1 \sqrt{\sigma / \mu}. \qquad (6)$$

Solving equation (1) under the boundary conditions

$$u = 0 \text{ when } y = 0 \text{ and } u = U \text{ when } y = h_1$$

we have

$$u = \frac{h_1^2}{\mu M^2} \frac{dp}{dx} \left[\cosh \frac{My}{h_1} - 1 - \frac{\cosh M - 1}{\sinh M} \sinh \frac{My}{h_1} \right] + U \frac{\sinh \frac{My}{h_1}}{\sinh M} \qquad (7)$$

Equations (3) - (5) yield

$$\frac{\partial}{\partial x} \left(\frac{1}{c^2} \frac{\partial P}{\partial x} \right) + \frac{\partial^2 P}{\partial y^2} = 0 \qquad (8)$$

Integrating equation (8) with respect to y from - H to 0, using the Morgan-Cameron approximation and remembering that $\left(\frac{\partial P}{\partial y} \right) = 0$ when $y = - H$, we have as in [10],

$$\left(\frac{\partial P}{\partial y} \right)_{y=0} = - H \frac{d}{dx} \left(\frac{1}{c^2} \frac{dp}{dx} \right) \tag{9}$$

Since the velocity component in the y-direction is continuous at the interface of fluid-film and porous matrix, we have

$$v_0 = V_{0y} = - \frac{k}{\mu} \left(\frac{\partial P}{\partial y} \right)_{y=0} , \tag{10}$$

using equation (4).

Integration of equation (2) across the film thickness yields

$$\frac{\partial}{\partial x} \int_0^{h_1} u \, dy - v_0 = 0 \tag{11}$$

Substituting equations (7), (9) and (10) into equation (11) we have

$$\frac{d}{dx}\left[\frac{dp}{dx}\left\{\frac{kH}{c^2} - \frac{h_1^3}{M^3}\left(2\tanh\frac{M}{2} - M\right)\right\}\right]$$

$$= \mu U h_1 \frac{d}{dx}\left(\frac{\tanh\frac{M}{2}}{M}\right). \tag{12}$$

Using the following dimensionless quantities

$$\bar{p} = \frac{h_1^2 p}{\mu U A}, \quad \bar{x} = \frac{x}{A} \text{ and } \psi = \frac{kH}{h_1^3}. \tag{13}$$

in equation (12) and integrating it once, we have

$$\frac{d\bar{p}}{d\bar{x}} = \frac{M^3 Q - M^2 \tanh M/2}{2\tanh M/2 - M - M^3\psi/c^2}, \tag{14}$$

where Q is the constant of integration.

The boundary conditions on $\bar{p}$ are

$$\bar{p}(0) = \bar{p}(1) = 0. \tag{15}$$

Integration of equation (14), using (15), yields

$$\bar{p} = Q \int_0^{\bar{x}} \frac{M^3 \, d\bar{x}}{2 \tanh M/2 - M - M^3 \psi / c^2}$$

$$- \int_0^{\bar{x}} \frac{M^2 \tanh M/2 \quad d\bar{x}}{2 \tanh M/2 - M - M^3 \psi / c^2} , \qquad (16)$$

where

$$Q = \frac{\int_0^1 \frac{M^2 \tanh M/2 \quad d\bar{x}}{2 \tanh M/2 - M - M^3 \psi / c^2}}{\int_0^1 \frac{M^3 \, d\bar{x}}{2 \tanh M/2 - M - M^3 \psi / c^2}} \qquad (17)$$

The dimensionless load capacity of the bearing is

$$\bar{W} = \frac{h_1^2 \, W}{\mu U A^2 B} = \int_0^1 \bar{p} \, d\bar{x} \qquad (18)$$

which is obtained as

$$\bar{W} = \int_0^1 \frac{M^2 \tanh M/2 \quad \bar{x} \, d\bar{x}}{2 \tanh M/2 - M - M^3 \psi / c^2}$$

$$- Q \int_0^1 \frac{M^3 \, \bar{x} \, d\bar{x}}{2 \tanh M/2 - M - M^3 \psi / c^2} \qquad (19)$$

The frictional force on the slider is

$$F = B \int_0^A \mu \left(\frac{\partial u}{\partial y} \right)_{y=h_1} dx \qquad (20)$$

and in dimensionless form it is

$$\bar{F} = \frac{h_1 F}{\mu U A B}$$

$$= \int_0^1 \left[M \coth M + \frac{M^2 Q \tanh M/2 - M\tanh^2 M/2}{2 \tanh M/2 - M - M^3 \psi / c^2} \right]$$

$$\cdot \, d\bar{x} \qquad (21)$$

4.2 Optimum profile

Following the method of Kuzma [52], we have

$$\delta \bar{W} = \int_0^1 f(\bar{x}) \left[\bar{x} - \frac{\int_0^1 \bar{x} \, g(\bar{x}) \, d\bar{x}}{\int_0^1 g(\bar{x}) \, d\bar{x}} \right] \delta M \, d\bar{x} \qquad (22)$$

where

$$f(\bar{x}) = \frac{d}{dM}\left[\frac{M^2 \tanh M/2}{2 \tanh M/2 - M - M^3\psi/c^2}\right]$$

$$- Q \frac{d}{dM}\left[\frac{M^3}{2 \tanh M/2 - M - M^3\psi/c^2}\right] \tag{23}$$

and

$$g(\bar{x}) = \frac{M^3}{2 \tanh M/2 - M - M^3\psi/c^2} . \tag{24}$$

From equations (22) and (23) we see that the optimum magnetic field profile is a step function with $M = 0$ on the lower step and M taking a fixed maximum value on the upper step. The location of the step $\bar{x} = s$ is given by

$$s = \frac{\int_0^1 \bar{x}\, g(\bar{x})\, d\bar{x}}{\int_0^1 g(\bar{x})\, d\bar{x}} . \tag{25}$$

For a given maximum value $\bar{M}$ of M, equations (24) and (25) are combined to give the following quadratic in s :

$$s\left[\frac{-12s}{1+12\psi} + (1-s)\beta^* \right] = -\frac{6s^2}{1+12\psi} + \frac{1-s^2}{2}\beta^* \qquad (26)$$

where β^* is the value of $g(\bar{x})$ when $M = \bar{M}$.

Thus

$$s = \frac{\beta^* + \sqrt{12(-\beta^*)/(1+12\psi)}}{[12/(1+12\psi)] + \beta^*} \qquad (27)$$

In the non-porous case, $\psi = 0$ and the results agree with those of Kuzma [52].

4.3 Results and discussion

For given $\bar{M}$ and ψ we compute s from equation (27), Q from (17) and then $\bar{W}$ and $\bar{F}$ from equations (19) and (21) respectively. The effects of $\bar{M}$ and ψ are expressed in tabular form.

Tables 15 and 16 show that both $\bar{W}$ and $\bar{F}$ decrease when ψ increases while they increase with $\bar{M}$.

That the friction factor increases with ψ while it decreases with $\bar{M}$ is shown by Table 17.

It is seen from Table 18 that the magnetic step location s can be increased either by increasing the permeability parameter or the maximum Hartmann number.

TABLE 15

Values of dimensionless load $\bar{W}$ for different values of $\bar{M}$ and ψ. $\frac{H}{h_1} = 0.02$ and $m^* = 0.6$

$\bar{M}$ \ ψ	0.000	0.001	0.010	0.100	1.000
10	1.399	1.382	1.278	0.745	0.156
20	1.992	1.968	1.803	0.993	0.190
30	2.266	2.239	2.043	1.100	0.203

TABLE 16

Values of dimensionless friction $\bar{F}$ for different values of $\bar{M}$ and ψ. $\frac{H}{h_1} = 0.02$ and $m^* = 0.6$

ψ / $\bar{M}$	0.000	0.001	0.010	0.100	1.000
10	4.248	4.236	4.072	3.160	1.842
20	5.474	5.454	5.191	3.800	2.004
30	6.026	6.001	5.689	4.067	2.065

TABLE 17

Values of Friction factor $\bar{F}/\bar{W}$ for different values of $\bar{M}$ and ψ. $\frac{H}{h_1} = 0.02$ and $m^* = 0.6$.

ψ / $\bar{M}$	0.000	0.001	0.010	0.100	1.000
10	3.037	3.065	3.187	4.245	11.781
20	2.748	2.771	2.879	3.826	10.556
30	2.659	2.680	2.784	3.698	10.193

Table 18

Values of magnetic field step location s for different values of $\bar{M}$ and ψ. $\frac{H}{h_1} = 0.02$ and $m^* = 0.6$.

ψ / $\bar{M}$	0.000	0.001	0.010	0.100	1.000
10	0.763	0.763	0.772	0.826	0.920
20	0.859	0.859	0.865	0.900	0.956
30	0.900	0.900	0.904	0.930	0.970